

Neutron-scattering experiments confirm the elastic model link between slow and fast dynamics of glass-forming liquids

Kristine Niss^{1,2}, Cécile Dalle-Ferrier¹, Bernhard Frick³, Daniela Russo³, Jeppe Dyre³ and Christiane Alba-Simionesco^{1,4}

¹*Laboratoire de Chimie Physique,
Bâtiment 349, Université Paris-Sud,
F-91405 Orsay, France*

²*DNRF centre “Glass and Time,
” IMFUFA, Department of Sciences,
Roskilde University, Postbox 260,
DK-4000 Roskilde, Denmark*

³*Institut Laue-Langevin,
F-38042 Grenoble, France.*

⁴*Laboratoire Léon Brillouin,
UMR 12, CEA-CNRS,
91191-Gif-sur-Yvette, France.*

(Dated: April 3, 2019)

Abstract

Mean-square displacements (MSD) were measured by neutron scattering at various temperatures and pressures for a number of molecular liquids close to their glass transitions. We find that there is no universal value of the MSD at T_g as required by the conventional glass transition Lindemann criterion. The MSD is universal along the glass transition line, however, thus establishing an ‘intrinsic’ Lindemann criterion for the glass transition. Finally, the time-scale dependence of the MSD and the role of anharmonicities are discussed in view of the elastic model prediction connecting one-to-one the MSD’s temperature dependence to the fragility in the vicinity of the glass transition.

I. INTRODUCTION

A major challenge to current condensed-matter physics is to explain the apparently universal properties of supercooled liquids approaching the glass transition. In particular, there is still no agreement about what causes the dramatic “super-Arrhenius” increase of the liquid’s viscosity that upon cooling in many cases increases more than one decade for a temperature decrease of just 1%. The most popular model is the Adam-Gibbs entropy model¹ which relates the slowing down to an underlying phase transition; this model involves the notion of a growing length scale as the liquid is cooled towards the glass transition, a prediction that has only recently become experimentally accessible^{2,3}. Another approach is advocated by the so-called elastic models, the main ideas of which date back to a paper by Eyring and co-workers from 1943⁴. These models relate the activation energy to the viscous liquid’s short-time elastic properties^{5,6}. Thus, apparently paradoxical, properties of the liquid that can be probed on the pico- or nanosecond time scale should determine the slow molecular relaxations taking place over minutes or hours (depending on the viscosity). This paper validates this intriguing prediction by studying several liquids, some under varying pressure by means of quasi-elastic neutron scattering experiments providing the most direct measurement available of the mean-square displacement on short time scales.

The idea of a connection between the dynamics on time scales differing by ten or more orders of magnitude has also been put forward in other contexts. If correct, it emphasizes the fact that the glass-transition phenomenon involves an exceedingly large dynamical range – and that a full understanding of the glass-transition must encompass both fast and slow dynamics. Before proceeding to describe the experiment, we give examples of the ideas and results which point in this direction.

In 1992 it was observed by Buchenau and Zorn⁷ that there is a relation between the temperature dependence of the structural relaxation time and the temperature dependence of the mean-square displacement (MSD) observed on the nano-pico second time scale in selenium as determined by neutron scattering experiments. Since then, other groups found similar results, showing qualitatively that the larger the fragility is, the stronger is the temperature dependence of the MSD^{8,9,10,11,12,13,14}. In 1987 Hall and Wolynes¹⁵ theoretically discussed how the mean-square vibrational displacement con-

trols the relaxation time according to the expression $\tau \propto \exp(\text{Const.}/\langle u^2 \rangle)$. Their approach was later developed into the random first-order transition theory (RFOT) of the glass transition^{16,17} where a variational density profile built of Gaussian vibrational displacements around aperiodic atomic positions is optimized for free-energy minimization. Thus the vibrational short-time displacement is the crucial quantity for the RFOT, which was later developed into a full-fledged theory that reproduces the famous Adam-Gibbs prediction for the relaxation time in terms of the configurational entropy¹.

In more recent works^{18,19} Novikov and Sokolov demonstrated a surprising connection between the “fragility” – a measure of how fast the liquid’s viscosity (or relaxation time) increases as temperature decreases and enters the glassy state – and elastic properties of the glass: The more fragile the liquid is, the higher is the ratio between the bulk and shear moduli of the resulting glass. Novikov and Sokolov discussed a possible explanation of this in terms of elastic models like the shoving model⁵. These authors also introduced a parameter derived from the measured dynamic structure factor, which relates the strength of the quasielastic scattering intensity at T_g normalized to the intensity of the boson peak and the fragility²⁰. The main point to be noted here is that the Novikov-Sokolov correlation provides an intriguing connection between short- and long-time properties of the liquid (since the liquid’s short-time mechanical properties are those of the glass corresponding to the liquid structure at the temperature in question).

Widmer and Harrowell²¹ proposed studying the Maxwell-Boltzmann ensemble averaged mean-squared displacement of a particle for any given initial configuration (the “iso-configurational ensemble”), terming this quantity the dynamic propensity of the particle in question. This property’s distribution reflects the dynamic heterogeneity of the liquid. Thus, once again, a connection is established between the long-time dynamic properties and MSD on time scales much shorter than the relaxation time.

Recently Leporini and collaborators²² argued from simulations as well as experiment that there is a universal correlation between the structural relaxation time and the “rattling amplitude” from high- to low-viscosity states. According to this picture the glass softens when the rattling amplitude exceeds a critical value. This implies a “universal” Lindemann criterion for the glass transition, i.e., that the glass transition takes place when the MSD reaches a certain value (see e.g. Ref. 6). Our results reported below do not confirm such a universal Lindemann criterion

At first sight it appear very surprising that there could be any relation between the alpha-relaxation process – taking place on the second or hour time scale – and mean-square displacements taking place on the nano-pico second time scale. It should be recalled, however, that whereas the alpha relaxation is very slow, the barrier transitions themselves are fast. This fact is the starting point for the elastic models. In these models the relation between mean-square displacement and fragility comes very natural, and the stiffness of the material or, equivalently, the steepness of the energy minima, determines the activation energy of the alpha process^{4,6,15}.

In terms of the vibrational MSD $\langle u^2 \rangle$, in the simplest version where the instantaneous bulk and shear moduli are proportional in their temperature variation, all elastic models imply for the activation energy $\Delta E(T) \propto Ta^2 / \langle u^2 \rangle$ at atmospheric pressure, where a is the average intermolecular distance^{6,12,15,23}. This implies

$$\tau(T) = \tau_0 \exp \left(\frac{Ca^2}{\langle u^2 \rangle(T)} \right), \quad (1)$$

where C is a constant. This result relates a larger MSD to a shorter alpha relaxation time. Hence elastic models predict that the change of the MSD just above T_g is more dramatic the more fragile the liquid is. This agrees with the generally observed trend, although questions remain about at which time scale $\langle u^2 \rangle$ should be considered. The glass transition Lindemann criterion states that the $\langle u^2 \rangle / a^2$, i.e., the relative vibrational amplitude of the atoms, at the glass transition should reach a certain universal value allowing diffusion on long time and length scales^{6,27,28}. Recall that the Lindemann criterion is the rule that $\langle u^2 \rangle / a^2 \sim 1\%$ when any crystal melts. If the glass transition is also characterized by such a universal number, there would be an appealing analogue between crystal and glass “melting” – although the latter phenomenon is known to be cooling rate dependent.

In this paper we present a *quantitative* test of Eq. (1) based on MSD data in the nano- and pico-second time scale obtained by neutron backscattering and time-of-flight techniques on several molecular liquids, covering fragilities ranging from 49 to 150. Three liquids were also studied under varying pressure. This allows one to examine different glass transitions of the same liquid, i.e., without changing the intermolecular interactions.

II. EXPERIMENTAL

The experiments were carried out on the back-scattering instruments IN10 and IN16 at ILL. The wavelength of the neutrons was 6.27 Å. The monochromation was done using the (1 1 1) reflection of Si yielding an energy resolution of FWHM=1 μeV (corresponding to a time scale of ~ 4 ns). The Q range covered was 0.2\AA^{-1} to 2\AA^{-1} . The experiments were performed isobarically in cooling with a rate of ~ 0.5 K/min. Pressure was applied using a clamp pressure cell mounted on the bottom of an insert to the cryostat. Sample transmission was 88% for the high-pressure measurements and 95% for the measurements at atmospheric pressure in standard aluminium cells. There is smaller transmission of the high-pressure measurements because more sample is needed to get a reasonable signal to noise ratio, when using the rather heavy pressure cell. The liquids studied are: glycerol, cumene, dibutylthalate (DBP), m-toluidine, sorbitol, triphenylphosphite (TPP) and decahydroisoquinoline (DHIQ). The first three were also studied at elevated pressure (300 MPa or 500 MPa); the pressure dependence of the glass-transition temperature was obtained from calorimetric experiments or extracted from dielectric spectroscopy under pressure^{24,25}. The preliminary data treatment was performed using the standard ILL software Sqwel. The MSD is calculated from the measured elastic intensities by adopting the Gaussian approximation, $\ln(I) = A - \frac{Q^2 \langle u^2 \rangle}{3}$ with A being a constant. We find that this Q^2 dependence is obeyed in the temperature range 0 K to $1.2 T_g$.

Supplementary experiments on DHIQ and DBP were carried out on the back-scattering instrument IN13. The energy resolution on IN13 is almost ten times wider, FWHM=8 μeV , meaning that the MSD we access in the measurement is probed on an almost 10 times faster time scale (~ 0.5 ns).

III. THE LINDEMANN CRITERION

Our measurements give the molecular MSD at the nano and the picosecond time scale. How can the elastic model prediction be tested? Comparing data for the same liquid at differing pressures, avoids making assumptions about the constant C . If it turns out that C is common to all liquid, a universal (i.e., genuine) glass transition Lindemann criterion is implied.

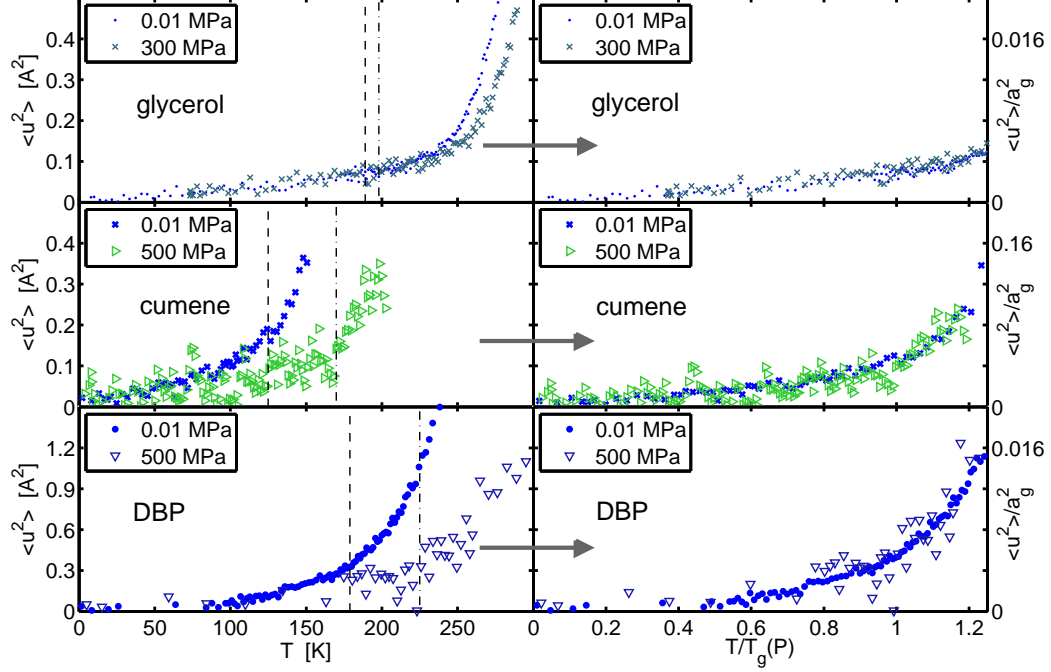


FIG. 1: The MSD of glycerol, cumene and DBP at atmospheric pressure and at 500 MPa (300 MPa for glycerol). The left hand side of the figure shows $\langle u^2 \rangle$ and temperature on an absolute scale. The dashed lines indicate T_g , the dash-dotted lines T_g at high pressure. The temperature scale in the right hand side of the figure is scaled by the pressure dependent T_g and the y-axis is scaled with $a^2 \propto \rho^{-2/3}$ evaluated at $(T_g(P), P)$.

In Fig. 1 we present data for three liquids (glycerol, cumene, and dibutylphthalate) studied at ambient as well as at high pressures (300 MPa for glycerol, 500 MPa for the two other liquids). The intermolecular distance scales with density as $a \propto \rho^{-1/3}$. The left part of each figure give the mean-square displacement as function of temperature at the two pressures where the dashed line marks the glass transition temperature. The right part gives the data scaled as implied by Eq. (1), giving $\langle u^2 \rangle(T)/a^2$ as a function of T/T_g with $a^2 \propto \rho^{-2/3}$ evaluated at $(T_g(P), P)$ from known equations of state^{24,25}. For all three liquids there is data collapse, showing that a Lindemann type criterion is fulfilled²⁶.

The next step is to investigate whether the constant C in Eq. 1 is common to all liquids, as required by a universal glass-transition Lindemann criterion^{5,22}. This is investigated in Fig. 2 by plotting $\langle u^2 \rangle(T)/a^2$ as function of T/T_g for a selection of liquids for clarity at ambient pressure with quite similar T_g 's. If the constant C were universal, $a^2/\langle u^2 \rangle$ should be the same for all liquids at T_g . The figure shows that this is not the case since

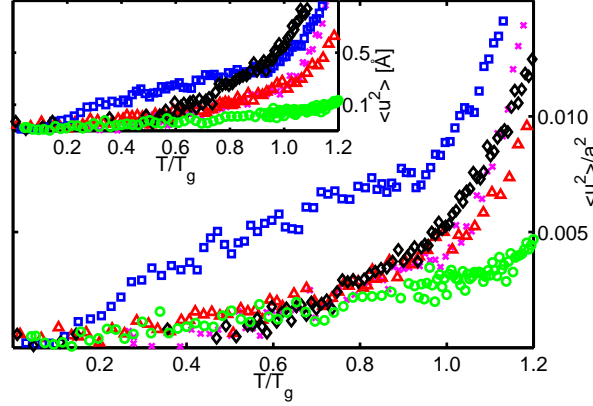


FIG. 2: The temperature dependence of $\langle u^2 \rangle$ scaled to $a^2 = v^{2/3}$ (see text for details) for 5 different liquids; glycerol (circles), DBP (diamonds), m-toluidine (squares), cumene (triangles), DHIQ (crosses). The temperature is scaled to T_g . The inset: The same data as in the main figure, here shown with the absolute value of $\langle u^2 \rangle$.

the number $\langle u^2 \rangle(T_g)/a^2$ varies a factor of 3 going from glycerol to m-toluidine. It should be noted, though, that the temperature dependence of the MSD of m-toluidine has a strong increase far below T_g . This type of behavior has earlier has been seen in other systems and is associated with the methyl-group rotation. The $\langle u^2 \rangle$ of m-toluidine at T_g is therefore not directly related to the vibrations, as it is the case when any extra processes enter the experimental time window. Even for the four other liquids there is a factor 2 in variation when comparing $\langle u^2 \rangle(T_g)/a^2$, which can not be reduced by any *ad hoc* numbers (as beads), and we conclude that there is no universal Lindemann criterion.

IV. TEMPERATURE DEPENDENCE OF THE MSD ABOVE T_g

Figure 3 shows $\langle u^2 \rangle(T)/\langle u^2 \rangle_{T_g}$ as a function of T/T_g . The $\langle u^2 \rangle$ value of the very fragile liquid DHIQ at the nanosecond rises most, the $\langle u^2 \rangle$ of glycerol least, dramatically; the three remaining liquids, which all have similar intermediate fragilities, fall in between. The systems studied hence confirm the general trend that more fragile liquids have more temperature dependent MSD above T_g than do less fragile¹². The elastic models make a quantitative prediction regarding the relation between the temperature dependence of $\langle u^2 \rangle$ and that of the alpha relaxation time. Thus the elastic model leading to Eq. (1) is based on

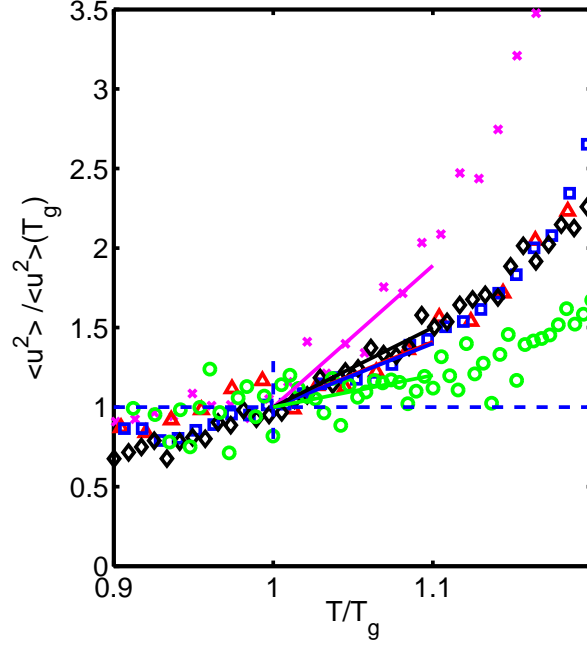


FIG. 3: The measured $\langle u^2 \rangle$ scaled to $\langle u^2 \rangle_{T_g}$ for 5 different liquids. The temperature is scaled to T_g . glycerol (circles), DBP (diamonds), m-toluidine (squares), cumene (triangles), DHIQ (crosses). The lines above T_g illustrate the fitted slopes used in Fig. 4.

$$\frac{\Delta E(\rho, T)}{k_B T} = \frac{Ca^2}{\langle u^2 \rangle(\rho, T)}. \quad (2)$$

Introducing the (isobaric) “activation energy index”²⁹ $I_P = - \left. \frac{d \ln \Delta E(T, \rho)}{d \ln T} \right|_P$ it follows that the elastic models predict (where the weak temperature dependence of a at constant pressure is ignored)

$$I_P = -1 + \left. \frac{d \ln \langle u^2 \rangle}{d \ln T} \right|_P. \quad (3)$$

Using the general relation⁶ between the conventional fragility index and I it follows that the model predicts a proportionality between Angell’s (isobaric) fragility m_P and the relative change of $\langle u^2 \rangle$ with relative change in temperature:

$$m_P = \log_{10} \left(\frac{\tau_g}{\tau_0} \right) (1 + I_P) = \log_{10} \left(\frac{\tau_g}{\tau_0} \right) \left. \frac{d \ln \langle u^2 \rangle}{d \ln T} \right|_P, \quad (4)$$

where $\tau_0 = 10^{-14}$ s is the microscopic time and $\tau_g = 100$ s is the relaxation time at the glass transition temperature (where fragility is evaluated). Hence the elastic model predicts a

correspondence between the slope seen in Fig. 2 at T_g and the fragility found from the temperature dependence of the alpha relaxation time.

Figure 4 tests this relation using fragilities and T_g 's taken from literature (see table IV for values and references). The value of $\frac{d \ln \langle u^2 \rangle}{d \ln T} |_P(T = T_g)$ in all cases is calculated in the temperature range from T_g to $\sim 1.1 T_g$, corresponding to the range where the fragility is determined. The data taken on the nanosecond time scale all lie close to the line. This result is rather convincing, especially because Eq. (4) not only predict that there is a proportionality between m_P and $\frac{d \ln \langle u^2 \rangle}{d \ln T} |_P(T = T_g)$, but the value of the proportionality constant as well.

The finding of Fig. 4 is consistent with another phenomenological feature observed in the dynamic structure factor as measured from inelastic scattering, suggesting that the relative strength of the boson peak compared to the fast relaxation, measured at T_g is related to the isobaric fragility of the glass former: a parameter, R , is defined as the quasielastic intensity divided by the boson peak intensity, and proposed to increase with increasing isobaric fragility. This model-independent assertion made by comparing the behavior of different glass formers^{19,20,30} holds pretty well but remains unexplained. Our findings re clearly consisten with this observation, showing the importance of fast processes at few nanosecond for the most fragile liquids and confirming that the boson peak intensity itself is not the relevant quantity for the correlation.

Compound	m_P	Refs.	$\frac{d \ln \langle u^2 \rangle}{d \ln T}$	$\frac{d \ln \langle u^2 \rangle}{d \ln T}$ fast	Refs.
glycerol	40, 53, 54	^{31, 32, 33}	2	1	this work ⁴²
DBP	75	³⁴	5	1.6	this work
<i>o</i> -terphenyl	82, 81, 76, 84	^{31, 43, 44, 45}	3.4*		¹⁰
<i>m</i> -toluidine	79,84	^{35, 36}	4		this work
cumene	90*	³⁷	4.1		this work
TPP	92*	⁴⁶	6		this work
sorbitol	100	⁴⁷	4.8		this work
DHIQ	158,163*	^{38, 40}	6	2.2	this work

TABLE I: Values and references for the points shown in figure 4. The asterisk indicates that the value has been calculated from data in the paper. .

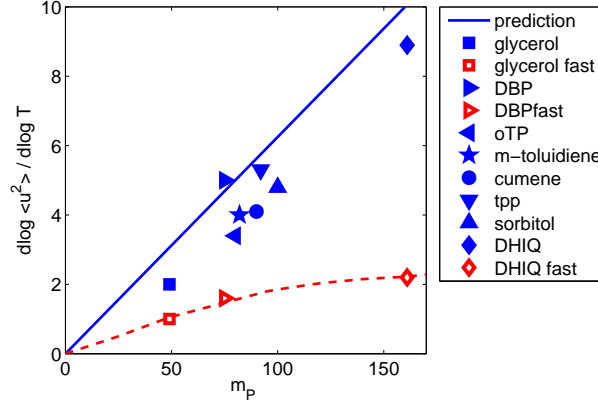


FIG. 4: The value of $\left. \frac{\partial \ln \langle u^2 \rangle}{\partial \ln T} \right|_P$ as a function of the isobaric fragility. Full symbols (blue) are data that refer to the nanosecond time scale (~ 4 ns), open symbols (red) are data obtained on IN13 on a ten times faster time scale (~ 0.4 ns). The blue line shows the expression Eq. (4) which follows from assuming $\Delta E(T) \propto T / \langle u^2 \rangle$ as it predicted from the elastic model (using $\tau_g = 100$ s and $\tau_0 = 10^{-14}$ s.). Values and references are given in table IV. The points calculated at ~ 4 ns fall close to the predicted line, while the points calculated at ~ 0.4 ns where the $\langle u^2 \rangle$ is less influenced by relaxations fall much below the line (the red dotted curve is a guide to the eye). When points lie below the blue line, the temperature dependence of $\langle u^2 \rangle$ underestimates the temperature dependence of the activation energy. It should be noted that both x and y variables have considerable uncertainty as they are arrived at as numerical derivatives of data.

V. THE ROLE OF RELAXATIONS AND ANHARMONICITY

Although Fig. 4 shows an overall agreement with the elastic model prediction, a number of issues remain to be considered. Not only, of course, is a more extensive study of different liquids needed, there are also other more fundamental issues. One problem is that in elastic models it is usually assumed that the measured $\langle u^2 \rangle$ is purely vibrational, i.e., that no relaxational motion contributes to $\langle u^2 \rangle$ around T_g . It is not likely that this assumption is generally correct, however. Thus we know from time-of-flight spectra that DHIQ has a strong quasi-elastic scattering already at T_g ²⁴. Time-of-flight measurements have a broader resolution function, and consequently shorter time scale, so this quasi-elastic scattering corresponds to relaxation at even shorter times than the MSD probed by backscattering. The alpha relaxation itself also enters the experimental window at some time, possibly already when $\tau_\alpha \sim 1 \mu\text{s}$ if the relaxation function is very stretched.

This happens intrinsically faster for fragile liquids than for strong liquids (for which, also, the relaxation functions are generally actually less stretched).

To investigate the role of relaxations further we have performed supplementary measurements of the MSD of DHIQ and DBP (for glycerol we used literature data⁴² referring to the same timescale) using IN13 which has a broader than IN10 resolution and therefore accesses $\langle u^2 \rangle$ on a time scale which is approximately 10 times shorter. In Fig. 5 we compare the mean square displacement of DHIQ found on the two different instruments, two distinct timescales. The measured $\langle u^2 \rangle$ follow each other below T_g , which strongly indicates that we probe genuine vibrations in this regime and therefore that the finding of the Lindemann criterion is related to the vibrations, as predicted by the elastic models. Above T_g , on the other hand, we see a separation of the two curves. It is evident that the temperature dependence of the MSD on the nanosecond timescale probed by IN10 is much more pronounced than the temperature dependence on the shorter time scale probed by IN13. This dependence on the timescale indicates that we are not probing the purely vibrational MSD on the nanosecond time scale, but rather a combination of vibration and fast relaxations.

To describe the role of relaxations we adopt a “jump-diffusion” type modelling⁴¹: If on the time scale set by the experiment some molecules vibrate whereas others jump once or more, the MSD separates into two contributions: $\langle u^2 \rangle = \langle u^2 \rangle_{\text{vib}} + \langle u^2 \rangle_{\text{jump}}$. For the log-log derivatives one finds $d \ln \langle u^2 \rangle / d \ln T = A d \ln \langle u^2 \rangle_{\text{vib}} / d \ln T + B d \ln \langle u^2 \rangle_{\text{jump}} / d \ln T$ where $A = \langle u^2 \rangle_{\text{vib}} / \langle u^2 \rangle$ and $B = \langle u^2 \rangle_{\text{jump}} / \langle u^2 \rangle$ give the relative weights of the two contributions ($A + B = 1$). The jump contribution is most likely strongly temperature dependent. Thus any correction for this in order to get the pure elastic contribution to $d \ln \langle u^2 \rangle / d \ln T$ pushes the points in Fig. 4 downwards, i.e., further away from the line. This is exactly what we see for the $d \ln \langle u^2 \rangle / d \ln T$ obtained from the IN13 data on DHIQ, which is also shown in the Fig. 4. Similarly we see that the $d \ln \langle u^2 \rangle / d \ln T$ calculated from glycerol data taken on IN13 reported by Wuttke⁴² lie below the line. However, the difference between the two timescales is much less dominant for glycerol than for the very fragile DHIQ indicating the relaxation are more dominant in the latter.

Based on the above considerations, we conclude that using the vibrational part of the MSD as devised by the elastic models (Eq. (1)) underestimates the temperature dependence of the activation energy. The reason for this could be that Eq. 1 based on a simpli-

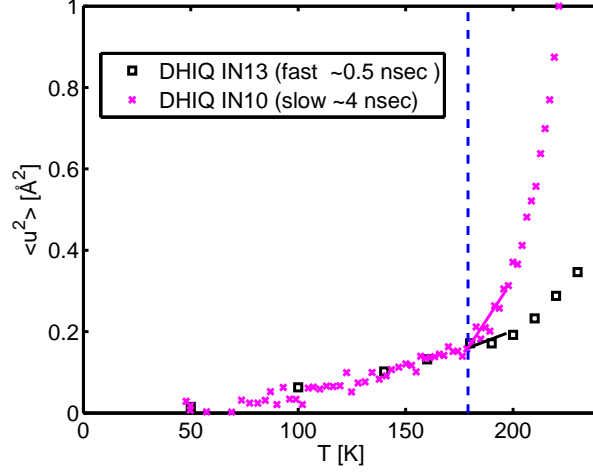


FIG. 5: The MSD of DHIQ measured by IN13 (on a time scale of ~ 0.4 nsec) and IN10 (on a time scale of ~ 4 nsec). The dashed lines indicate T_g . The lines above T_g illustrate the fitted slopes used in Fig. 4. The temperature dependence of the MSD is time scale independent below T_g while it becomes strongly time scale dependent above T_g . This indicates that $\langle u^2 \rangle$ below T_g is dominated by vibrations while relaxations play a role on the nanosecond time scale in the liquid above T_g (even close to T_g where the alpha relaxation time is still on the order of seconds).

fied reasoning that basically ignores anharmonicities⁶. There are two nontrivial assumptions going into this reasoning: a) The harmonic approximation, according to which the curvature at the minimum is inversely proportional to $\langle u^2 \rangle$; b) The energy barrier being proportional to the curvature at the minimum, as it would be if the potential were parabolic and scale accordingly. The first approximation applies to a good approximation at sufficiently low temperatures and may well apply to highly viscous liquids because these have fairly large energy barriers. The second approximation implies that if the barrier goes to zero, so does the curvature. However, this is not necessarily the case. Thus the simple elastic model assumption that the barrier scales with curvature may break down. In summary, for a given temperature dependence of $\langle u^2 \rangle$ a more realistic model might well predict larger $d \ln \Delta E / d \ln T$ than predicted by the elastic models. This corresponds to lowering the slope of the theoretical line of Fig. 4. This might explain why the $d \ln \langle u^2 \rangle / d \ln T$ measured at short times where we expect vibrations to be dominant lie on the lower side of the line.

VI. DISCUSSION AND CONCLUSION

The liquids studied show no universal Lindemann criterion when we compare the MSD on the nanosecond time scale. Three of the liquids were also studied under pressure. They obey a pressure-dependent Lindemann criterion, as predicted by the elastic models. Thus the use of pressure reveals a connection which is probably masked by details in the molecular interactions and geometries when comparing different liquids and suggest the existence of an *intrinsic* Lindemann criterion for each substance.

Above T_g it appears that the elastic model prediction underestimates the activation energy temperature dependence. We suggest that these deviations are caused by anharmonic effects. In this context it should be noted that despite the simple “harmonic” appearance of the elastic models, anharmonicities must play a role, even in the simplest elastic models. Thus the effective, temperature-dependent elastic constant (or curvature at energy minima) reflects anharmonicity because in truly harmonic potentials the elastic constants are temperature independent.

While the vibrational part of the mean square displacement does not follow the prediction of the elastic models we find that the total mean square displacement measured, $\langle u^2 \rangle(T)$ at the nanosecond time scale (vibrations and relaxations) approximately follow a proportionality of the type $\Delta E(T) \propto T / \langle u^2 \rangle$, where $\Delta E(T)$ is the activation energy governing the alpha relaxation. This one-to-one finding is based on measurements of MSD on the nanosecond timescale by neutron scattering as function of temperature of molecular liquids covering a significant range of fragilities. The proportionality $\Delta E(T) \propto T / \langle u^2 \rangle$ shows that there is a connection between the fast and the slow dynamics close to the glass transition. It is not clear how casual is the relation, where the increase in mean square displacement leads to higher mobility and consequently a speed up of the alpha relaxation, or if the increased mean square displacement is a due to a precursor of alpha relaxation itself, for example as a high frequency von Schweidler regime.

To summarize we find (i) a Lindemann criterion for each liquid as predicted by the elastic models by studying the same liquids at different pressures; (ii) the temperature dependence of the MSD on the nanosecond time scale links to the liquid fragility as predicted by the elastic models; (iii) there is no universal glass-transition Lindemann criterion. These observations are rationalized by introducing an anharmonicity in the elastic

models, and they are fully consistent with other experimental features and correlations found in the literature. These findings show that a full understanding of the viscous slowing down and the glass transition must involve both the fast and the slow dynamics.

- ¹ G. Adam and J. H. Gibbs, J. Chem. Phys. **43**, 139 (1965).
- ² L. Berthier, G. Biroli, J-P. Bouchaud, L. Cipeletti, D. El Masri, D.L'Hôte, et al. Science **310**, 1797 (2005).
- ³ C. Dalle-Ferrier et al., Phys. Rev E **76**, 041510 (2007).
- ⁴ A. Tobolsky, R. E. Powell, and H. Eyring, in *Frontiers in Chemistry*, Vol. 1, edited by R.E. Burk and O. Grummit (Interscience, New York, 1943), p. 125.
- ⁵ J. C. Dyre, N. B. Olsen, and T. Christensen, Phys. Rev. B **53**, 2171 (1996).
- ⁶ J. C. Dyre, Rev. Mod. Phys. **78**, 953 (2006).
- ⁷ U. Buchenau and R. Zorn, Europhys. Lett. **18**, 523 (1992).
- ⁸ C. A. Angell, Science **267**, 1924 (1995).
- ⁹ T. Kanaya, T. Tsukushi, K. Kaji, J. Bartos, and J. Kristiak, Phys. Rev. E **60**, 1906 (1999).
- ¹⁰ R. Casalini and K. L. Ngai, J. Non-Cryst. Solids **293**, 318 (2001).
- ¹¹ S. Magazu, G. Maisano, F. Migliardo, and C. Mondelli, Biophys. J. **86**, 3241 (2004).
- ¹² K. L. Ngai, Phil. Mag. **84**, 1341 (2004).
- ¹³ K. L. Ngai, J. Non-Cryst. Solids **275**, 7 (2000).
- ¹⁴ E. Cornicchi, G. Onori, and A. Paciaroni, Phys. Rev. Lett. **95**, Art. No. 158104 (2005).
- ¹⁵ R. W. Hall and P. G. Wolynes, J. Chem. Phys. **86**, 2943 (1987).
- ¹⁶ X. Xia and P. G. Wolynes, Proc. Natl. Acad. Sci. USA **97**, 2990 (2000).
- ¹⁷ V. Lubchenko and P. G. Wolynes, Ann. Rev. Phys. Chem. **58**, 235 (2006).
- ¹⁸ V. N. Novikov and A. P. Sokolov, Nature **431**, 961 (2004).
- ¹⁹ V. N. Novikov, Y. Ding and A. P. Sokolov, Phys. Rev. E **71**, 061501 (2005).
- ²⁰ A. P. Sokolov, E. Rössler, A. Kisliuk, and D. Quitmann, Phys. Rev. Lett. **71**, 2062 (1993).
- ²¹ A. Widmer-Cooper and P. Harrowell, J. Phys.: Condens. Matter **17**, S4025 (2005).
- ²² L. Larini, A. Ottochian, C. De Michele, and D. Leporini, Nature Phys. **4**, 42 (2008).
- ²³ C. P. Flynn, Phys. Rev. **171**, 682 (1968); A. P. Sokolov, A. Kisliuk, D. Quitmann, A. Kudlik, and E. Rössler, J. Non-Cryst. Solids **172**, 138 (1994); C. M. Roland and K. L. Ngai, J. Chem. Phys. **104**,

- 2967 (1996); M. M. Teeter, A. Yamano, B. Stec, and U. Mohanty, *Proc. Natl. Acad. Sci. (USA)* **98**, 11242 (2001); F. W. Starr, S. Sastry, J. F. Douglas, and S. C. Glotzer, *Phys. Rev. Lett.* **89**, Art. No. 125501 (2002); P. Bordat, F. Affouard, M. Descamps, and K. L. Ngai, *Phys. Rev. Lett.* **93**, Art. No. 105502 (2004).
- ²⁴ K. Niss, Ph.D. thesis, Université de Paris XI (2007).
- ²⁵ C. Dalle-Ferrier, Ph.D. thesis, Université de Paris XI (2009).
- ²⁶ The scaling of the temperature axis is by far the most important for this data collapse. The estimated increase in density is less than 10%. This gives a decrease of a^2 by approximately 5%. This difference is almost indistinguishable in figure 1 due to the scatter of the data.
- ²⁷ U. Buchenau and A. Wischnewski, *Phys. Rev. B* **70**, 092201 (2004).
- ²⁸ B. Frick, D. Richter, W. Petry and U. Buchenau, *Zeitschr. fur Phys. B-cond. matt.* **70** 73 (1988); V. K. Malinovsky and V. N. Novikov, *J. Phys.: Condens. Matter* **4**, L139 (1992); A. Heuer and H. W. Spiess, *J. Non-Cryst. Solids* **176**, 294 (1994); V. N. Novikov, E. Rössler, V. K. Malinovsky, and N. V. Surovtsev, *Europhys. Lett.* **35**, 289 (1996); J. N. Onuchic, Z. Luthey-Schulten, and P. G. Wolynes, *Ann. Rev. Phys. Chem.* **48**, 545 (1997); D. S. Sanditov, S. S. Sangadiev, and G. V. Kozlov, *Glass Phys. Chem.* **24**, 539 (1998); X. Xia and P. G. Wolynes, *Proc. Natl. Acad. Sci. USA* **97**, 2990 (2000); V. N. Novikov and A. P. Sokolov, *Phys. Rev. E* **67**, Art. No. 031507 (2003); R.S. Berry and B. M. Smirnov *Phys. Usp.* **48**, 345 (2005).
- ²⁹ J. C. Dyre and N. B. Olsen, *Phys. Rev. E* **69**, 042501 (2004).
- ³⁰ K. Niss and C. Alba-Simionesco, *Phys. Rev. B* **74**, 024205 (2006).
- ³¹ C. Alba-Simionesco, A. Cailliaux, A. Alegria, and G. Tarjus, *Europhys. Lett.* **68**, 58 (2004).
- ³² N. O. Birge, *Phys. Rev. B* **34**, 1631 (1986).
- ³³ M. Paluch, R. Casalini, S. Hensel-Bielowka, and C. M. Roland, *J. Chem. Phys.* **116**, 9839 (2002).
- ³⁴ K. Niss, C. Dalle-ferrier, G. Tarjus, and C. Alba-Simionesco, *J. Phys-cond. Matt* **19**, 0953 (2007).
- ³⁵ C. Alba-Simionesco, J. Fan, and C. A. Angell, *J. Chem. Phys.* **110**, 5262 (1999).
- ³⁶ A. Mandanici, M. Cutroni, and R. Richert, *J. Chem. Phys.* **122**, 084508 (2005).
- ³⁷ A. J. Barlow, J. Lamb, and A. J. Matheson, *Proc. R. Soc. London A* **292**, 322 (1966).
- ³⁸ R. Richert, K. Duvvuri, and L. T. Duong, *J. Chem. Phys.* **118**, 1828 (2003).
- ³⁹ N. B. Olsen, *J. Non-Cryst. Solids* **235**, 399 (1998).
- ⁴⁰ R. Casalini, K. J. McGrath, and C. M. Roland, *J. Non-Cryst. Solids* **352**, 4905 (2006).
- ⁴¹ K. S. Singwi, A. SjolanderJOLANDER *Phys. Rev.* **119** 3, 863 (1960)

- ⁴² J. Wuttke, W. Petry, G. Coddens, F. Fujara, Phys. Rev. E, **52** 4026 (1995)
- ⁴³ P. K. Dixon and S. R. Nagel, Phys. Rev. Lett. **61**, 341 (1988).
- ⁴⁴ D. H. Huang and G. B. McKenna, J. Chem. Phys. **114**, 5621 (2001).
- ⁴⁵ M. Paluch, K. L. Ngai, and S. Hensel-Bielowka, J. Chem. Phys. **114**, 10872 (2001).
- ⁴⁶ N. B. Olsen, T. Christensen, and J. C. Dyre, Phys. Rev. Lett. **86**, 1271 (2001).
- ⁴⁷ N. B. Olsen, J. Non-Cryst. Solids **235**, 399 (1998)